Progress In Electromagnetics Research C, Vol. 126, 125–142, 2022

A High-Gain Dual-Band Superstates Enabled Antenna for 5G-mm Wave Applications

Aafreen Khan[1, *], Anwar Ahmad[1], and Maksud Alam[2]

Abstract—In this article, the antenna is designed by using different shapes of patch structures on $8.468 \times 9.741\,\text{mm}^2$ ground plane. Different shapes like A, H, F, T, and U are simulated by using HFSS Software. For gain enhancement, various techniques on the different shape patches have been applied. The maximum gain achieved in the case of A shape patch with MTM structure and circular reflector with superstates is 14.2 dBi, and the band covered is (36.248–38.764) GHz and (33.384–34.503) GHz. Other shapes like H, F, T, and U are designed by modification in A shape patch, and by applying various techniques like MTM and reflector surface with superstates interesting results have been achieved. The designed antenna is an mm-wave antenna and a novel structure for 5G communications.

1. INTRODUCTION

The evolution of technology plays an important role to overcome the challenges faced by users. Wireless technology is one of the revolutionary ones as it has given many benefits to society. So, in the journey of changing wired to wireless medium antenna plays a main role. Many types of antennas have been categorized, but microstrip patch antennas have an important role in various applications because of their compact size and easy structure design along with good performance parameters. Changing technology from 4G to 5G demands 5G antennas. 5G antenna design includes sub-6 GHz and mm-wave bands. Designing microstrip patch antennas for mm-wave bands has become an interesting part because of its various advantages. The designing of mm-wave antenna also has the hurdle of low gain as the increase in the frequency gets absorbed in the environment easily. So, designing antennas at mm-wave with a good gain is not an easy task. In the proposed article, a high gain antenna with different shape patches of A, H, F, T, and U has been designed with the implementation of MTM, reflector, and superstate technology, and the maximum gain achieved in the case of A-shape patch. The given antenna is a novel structure with dual band characteristics for mm-wave 5G applications.

In various reflector surface antennas like in stacked patch antennas, reflector element has been used to reduce backward radiation [1]. Also, the superstate implementation for directivity enhancement has been done in [2]. In the Fabry Perotantenna, array gain enhancement has been done by using a partial reflector surface (PRS) [3]. In the design of a reflectarray microstrip antenna, the reflect array has been used for beam switching and dual polarisation [4]. Also, in [5] holographic meta surface has been used which increases the radiation aperture that increases the antenna gain. In tri-band antenna combining transmitting array and reflector array, five-layer patches on three dielectric substrates have been used, and good antenna performance characteristics have been achieved [6]. In a coplanar waveguide (CPW)-fed monopole antenna, an artificial magnetic conductor (AMC) structure has been used as a reflector surface, and the gain with other performance parameters has been enhanced [7]. In negative metamaterial (MTM) microstrip antenna the gain enhancement has been achieved by using

Received 28 September 2022, Accepted 19 October 2022, Scheduled 3 November 2022

* Corresponding author: Aafreen Khan (aafreen.khan1994@gmail.com).

[1] Department of Electronics and Communication Engineering, Jamia Millia Islamia, India. [2] Department of Electronics and Communication Engineering, Galgotia College of Engineering and Technology, Greater Noida, India.

split-ring resonators (SRRs) structure [8]. In Vivaldi antennas, the directivity has been improved by using a zero index MTM structure [9]. In a 60 GHz slot antenna zero-index MTM (ZIM) enhances the gain of the antenna at high frequencies [10]. For gain improvement in [11], an electromagnetic bandgap structure (EBG) substrate has been used. In a log periodic antenna, the gain has been enhanced by using a non-resonant metamaterial structure [12]. In circularly polarised high gain antenna for gain enhancement PRS structure has been used [13]. In [14], the directivity has been enhanced, and beamwidth is controlled by using a low-profile metasurface. In high gain antenna systems for biomedical applications, the metamaterial and superstate with high permittivity have been used for gain enhancement [15]. In the proposed antenna design high gain, A-shape patch with reflector, and superstates have been designed which is novel in design and has the good performance characteristics useful for 5G mm-wave applications.

2. DESIGN PROCEDURE

The designed antenna is mounted on $8.468 \times 9.741\,\text{mm}^2$ ground plane. The height of the substrate is 0.8 mm. The substrate is made of RT-Duroide 5880 with the ε_r value of 2.2. Different shape patches have been mounted on the Duroide substrate. The radiating patch shape has the structure A shape, H

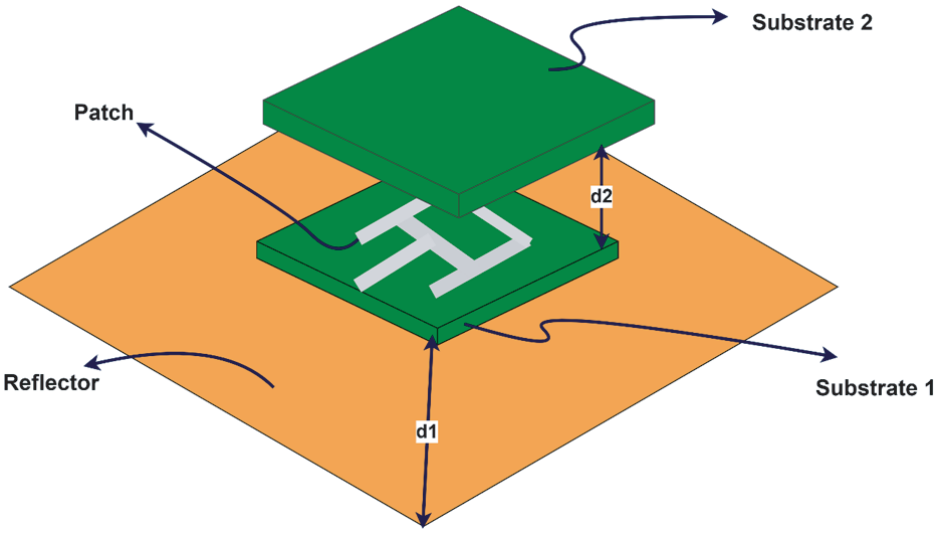

Figure 1. Isometric view of designed superstate antenna with reflector surface and MTM.

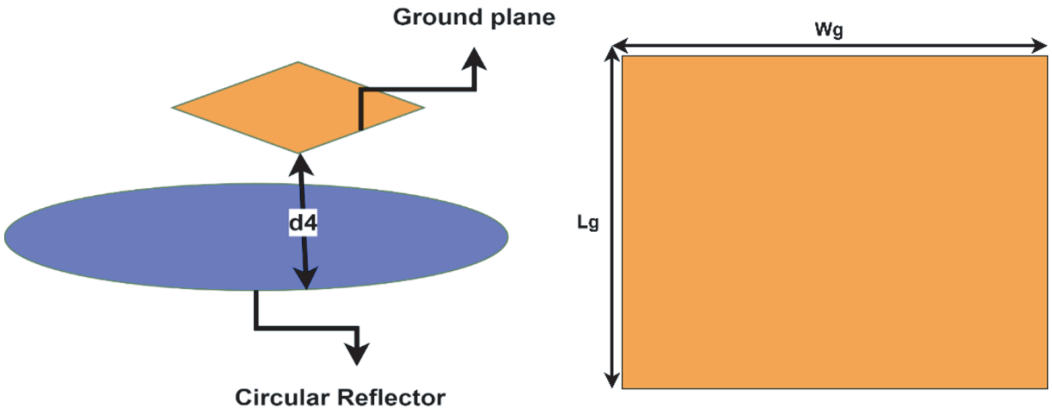

Figure 2. (a) Circular reflector implementation. (b) Bottom view of a ground plane.

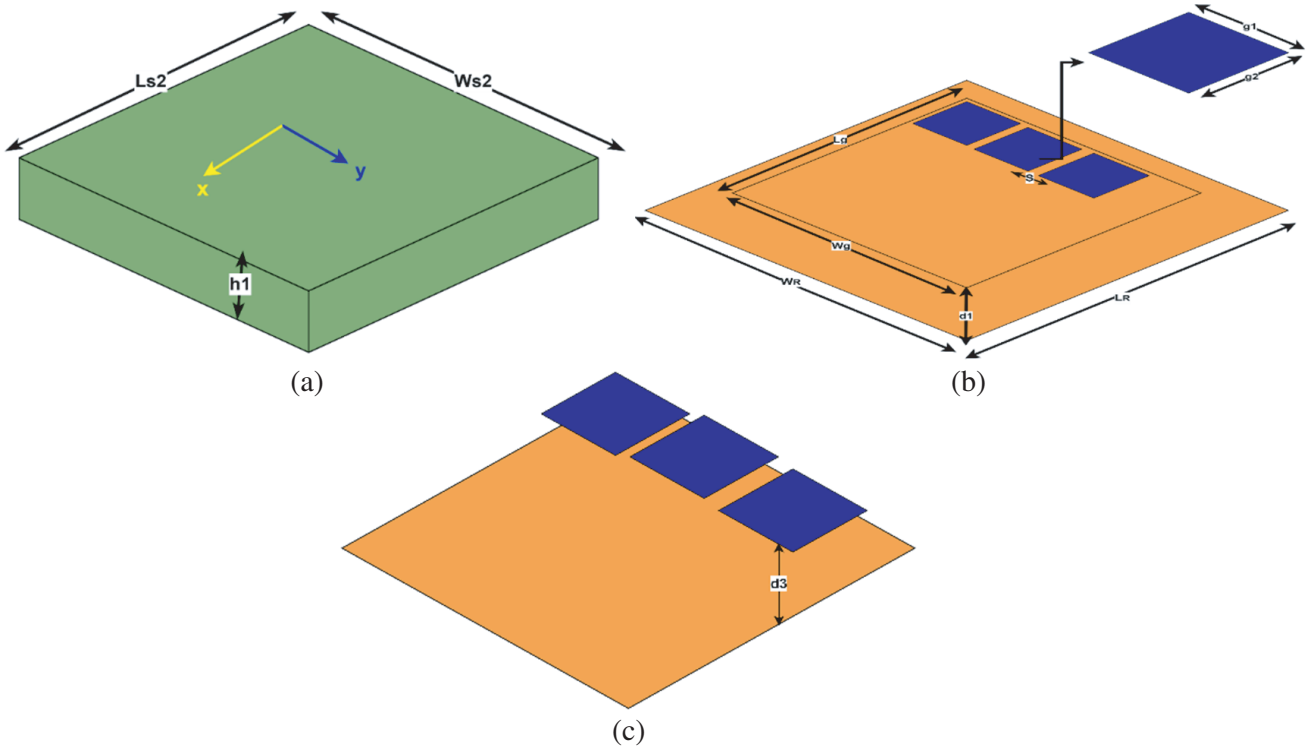

Figure 3. (a) Superstate. (b) MTM with unit cell structure and rectangle reflector. (c) MTM structure with ground plane.

shape, F shape, T shape, T shape modified, and U shape which has been represented in Figures 4(a), (b), (c), (d), (e), (f). All different shapes patches are firstly loaded with MTM structure, and the implemented MTM structure diagram is given in Figures 3(b), (c), to design an antenna with good performance parameters. A reflector surface of circular and rectangular shapes has been implemented. The circular shape reflector has a radius of 8 mm with a distance $d4$ from the ground plane which is shown in Figure 2(a), and the ground plane with the dimension is shown in Figure 2(b). The rectangular reflector of dimensions $16 \times 16\,\text{mm}^2$ has been implemented at the same distance $d4$. The implementation of different reflector surfaces changes the performance parameters. Another implementation of substrate that is called superstates has been done, and a change in the antenna performance parameter is analyzed. The superstate has a height of $h1 = 0.9$ mm, and the material used is silicon with a permittivity of 11. Figure 3(a) shows another substrate's dimensions. Also, the isometric view of the designed antenna is shown in Figure 1 with the MTM reflector and superstate implementation, and the dimensions of the proposed antenna are given in Table 1.

2.1. A Shape Patch

In the A-shape patch, the resonating frequency achieved is at 35.1310 GHz with the RL of -20.8661 dB, and the maximum gain achieved at 18.558 GHz is 7.7227 dBi. The top view of the A shape with substrate is given in Figure 5(a). The implementation of metamaterial structure (MTM) provides the resonating frequency of 38.2966 GHz (37.5912–38.938) GHz and 36.6207 GHz (36.506–36.681) GHz with the RL value of -17.5013 dB and -10.182 dB, respectively, and the maximum gain is 9.3421 dBi at 39.313 GHz. So, the enhancement in the gain has been obtained with the decrease in the RL value with the MTM structure, and the rectangular reflector resonates at the center frequency of 38.9483 GHz (36.7507–40.0446) GHz with the RL of -23.938 dB and maximum gain of 11.6981 dBi at 36.3414 GHz. So, the implementation of a rectangle surface enhances the RL and gain. The circular reflector is also added which resonates at 38.8552 GHz (37.134–39.597) GHz with an RL value of -21.7988 dB and maximum gain of 11.804 dBi at the resonating frequency of 37.272 GHz. Implementation of a

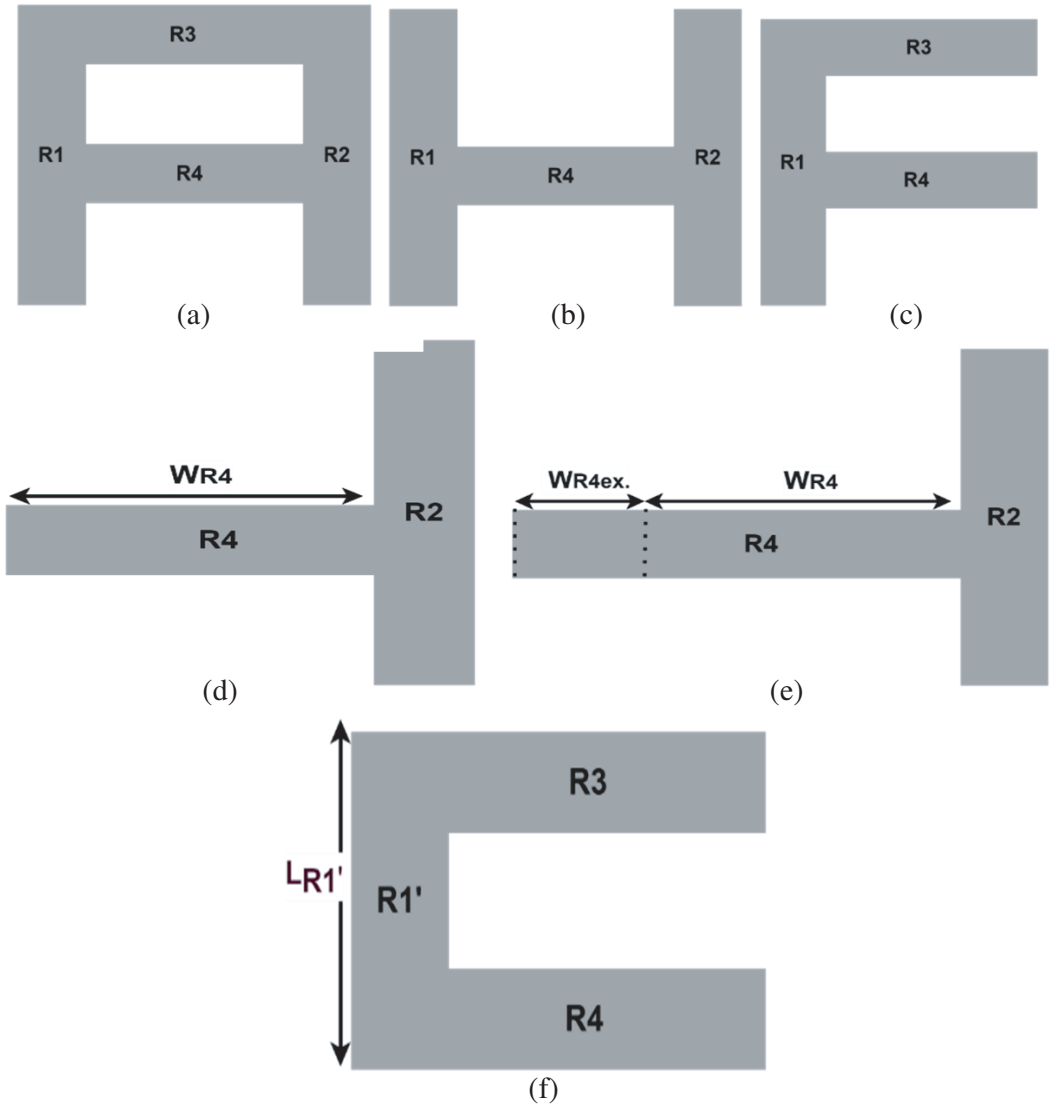

Figure 4. (a) A shape patch. (b) H-shape patch. (c) F-shape patch. (d) T-shape patch. (e) T-shape modified patch. (f) U-shape patch.

circular reflector surface also improves the gain of the antenna, and the RL value is also increased. The top view of the A shape patch with circular reflector is given in Figure 5(b). Now further with the reflector surface, the superstate of size $8.468 \times 9.741 \times 0.9\,\text{mm}^3$ has been implemented which is given in Figure 3(a). With the superstate implementation along with the MTM and rectangle reflector surface the antenna resonates at the center frequency of 36.806 GHz and 38.482 GHz with the RL −21.1736 dB and −16.1713 dB covering the band (36.0087–38.9816) GHz with the maximum gain value 14.13 dBi at resonating frequency 39.506 GHz, so the implementation of superstate enhances the gain of the antenna. In the further procedure, the same size superstate has been implemented with the circular reflector. The maximum gain achieved in this case is 14.202 dBi at 39.413 GHz with resonating frequency band 38.389 GHz, 37.086 GHz (36.248–38.764) GHz, and another band is 33.9207 (33.384–34.5033) GHz with the return loss −14.637 dB, −27.003 dB, −22.376 dB, respectively, which can be seen in Figures 6(a) and (b). The comparison of all methodologies is given in Table 2.

Table 1. Proposed antenna structure dimensions.

Dimensions	Value (mm)	Dimensions	Value (mm)
$WS1 = Ws2$	9.741	$D1$	1
$LS1 = LS2$	8.468	$D2$	3
$LR1$	4.5	$D3$	0.2
$LR2$	4.5	$D4$	1
$LR1'$	3.375	Lg	8.468
$WR3$	2.5	Wg	9.74
$WR4$	2.5	LR	8.468
$tR1$	1	WR	9.741
$tR2$	1	S	0.5
$tR3$	1	H	0.8
$tR4$	0.875	$H1$	0.9
R	8	$G1$	2
$Wr4ex$	2	$G2$	2

Table 2. Comparative performance parameter of A-shape patch.

Methodologies	Center frequency (GHz)	BW (GHz)	RL (dB)	Maximum Gain (dBi)
A shape	35.1310	2.3	−20.8661 dB	7.722
A shape+MTM	38.296, 36.620	1.3, 0.17	−17.501, −10.182	9.342
A shape+MTM+Circular Reflector	38.8552	2.462	−21.7988	11.804
A shape+MTM+Rectangular Reflector	38.948	3.29	−23.938	11.698
A shape+MTM+Rectangular Reflector+Superstates	36.806, 38.482	2.97	−21.173, −16.171	14.130
A shape+MTM+Circular Reflector+Superstates	37.086, 38.389, 33.384	2.51, 1.11	−27.003, −14.637, −22.376	14.202

2.2. H-Shape Patch

The H shape is derived from the A shape by removing $R3$ from the A shape. The simple H-shape patch is resonating at 35.5034 GHz (35.5034 GHz–36.8068 GHz) with RL −31.767 dB, and the maximum gain value is 7.8934 dB at 20.420 GHz. The MTM with H-shape is resonating at peak frequencies of 39.9724 GHz and 39.1345 GHz with the RL value of −35.4653 dB and −12.850 dB respectively. The bandwidth covered is (38.851–40.5446) GHz, and another resonating peak achieved is at 34.8517 GHz with the RL value of −14.7668 dB. The covered bandwidth is (33.7802–35.7814) GHz, and the maximum gain with the MTM is 8.3267 dBi at the 39.1345 GHz. In the H-shape patch when the same size circular reflector is implemented, the two resonating frequencies achieved are 39.693 GHz and 39.041 GHz (38.512–40.289) GHz with the RL values of −26.0626 dB and −17.038 dB. Also, the maximum gain achieved is 10.684 dBi at 39.4138 GHz. So implementing the circular reflector on the H-shape patch also increases the gain. When this circular reflector surface is replaced with the same size rectangular

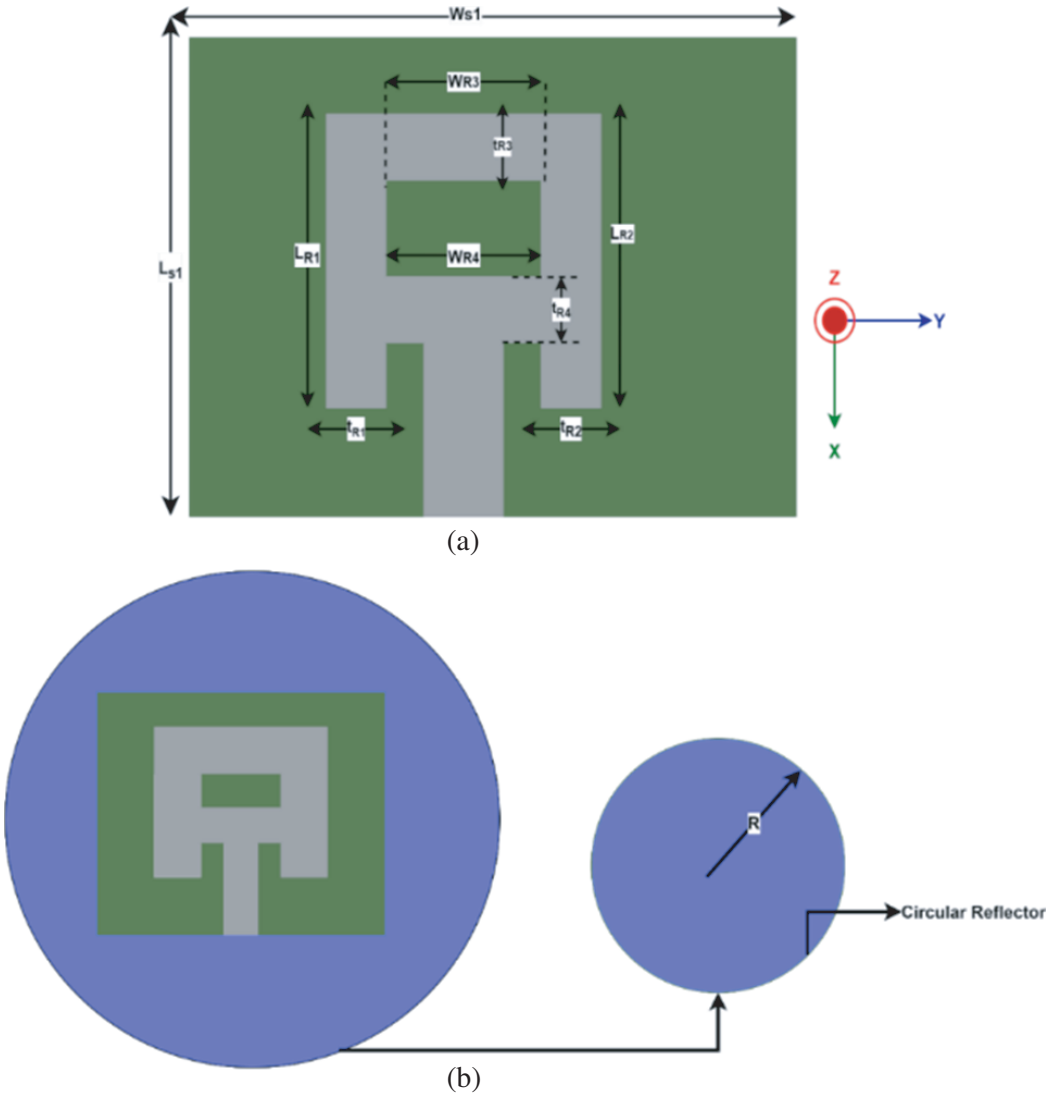

Figure 5. (a) Top view of A-shape patch with substrate. (b) Top view of A-shape with circular reflector.

reflector, the two resonating frequencies are 38.948 GHz (38.273–39.673) GHz and 34.572 GHz (33.6257–35.4581) GHz with the return loss value of −33.9303 dB and −14.40 dB respectively, and the maximum gain achieved is at 39.2241 GHz which is 10.8585 dBi. The rectangular reflector here increases the gain and return loss parameter. When another silicon substrate is added at $d2 = 3$ mm, the antenna resonates at three resonating frequencies which are 39.6 GHz with RL of −19.5090 dB and 39.227 GHz with RL value of −24.3265 dB, and the bandwidth covered is (38.5012–40.056) GHz. Another resonating frequency is 34.8517 GHz (34.1149–35.5335) GHz with the RL value of −14.8755 dB, and the maximum gain achieved is 12.6798 dBi at the resonating frequency of 40.1586 GHz. In another implementation of the same size superstate with the H-shape patch with a circular reflector, the resonating frequencies are 39.134 (38.4112–39.752) GHz and 34.758 GHz (34.161–35.494) GHz with RL −33.351 dB, −14.020 dB, respectively, and the maximum gain is 13.198 dBi at 39.693 GHz. A comparative H-shape RL and the gain plot are given in Figures 7(a) and (b). The comparative analysis of different methodologies implementation in H-shape patch is given in Table 3.

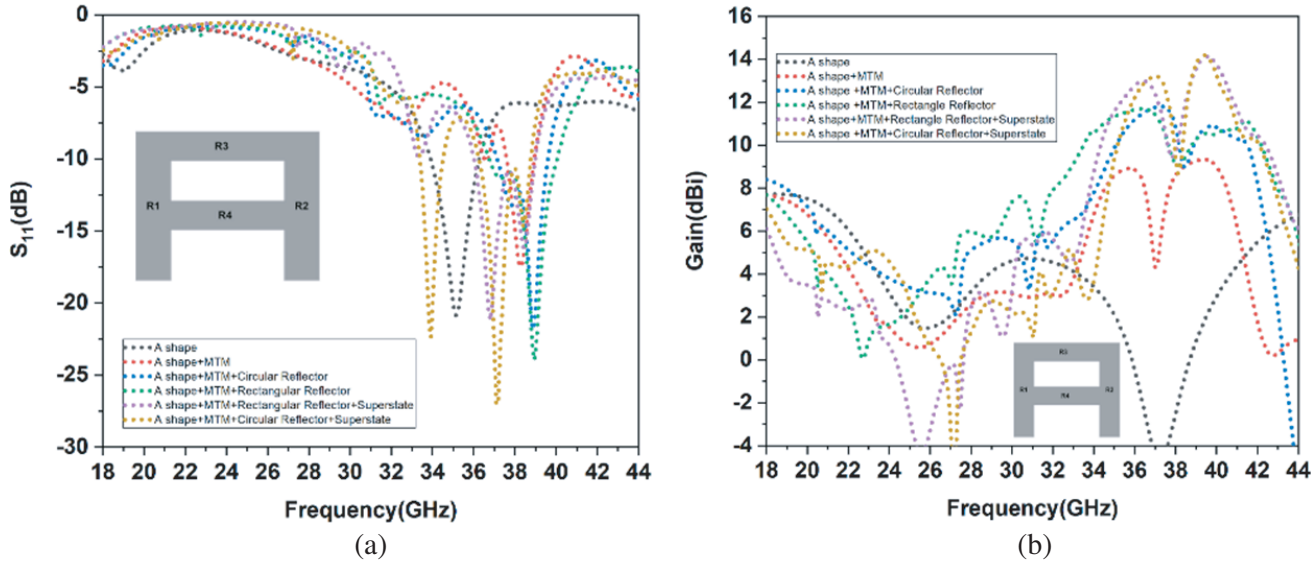

(a) (b)

Figure 6. (a) Return loss. (b) Gain of A shape patch antenna with all methodology implementation comparative.

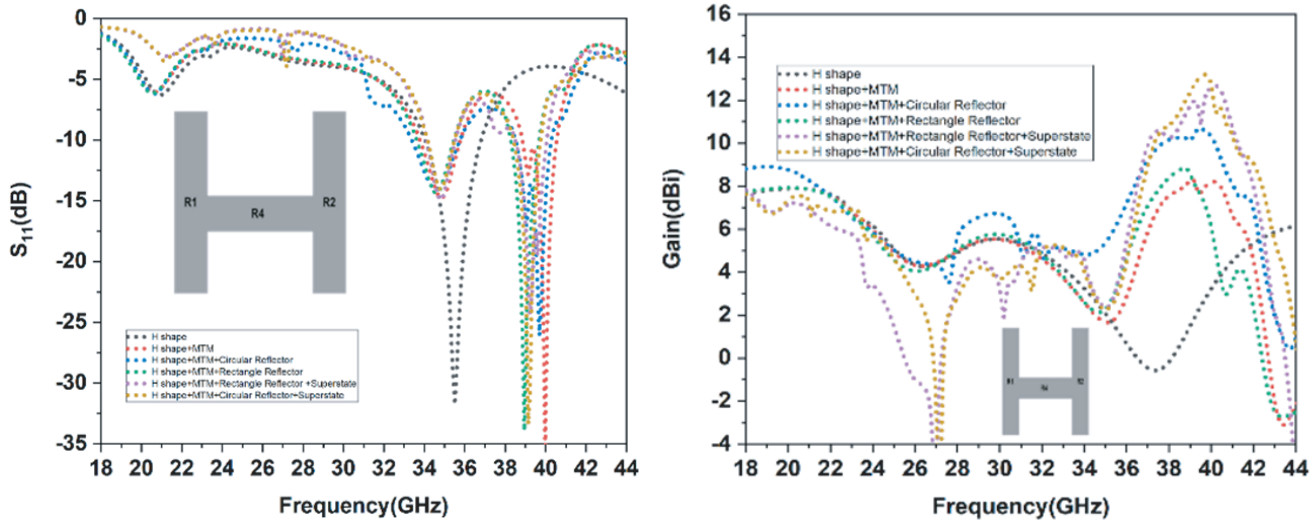

(a) (b)

Figure 7. (a) Return loss. (b) Gain of H-shape comparative with all methodology's implementation.

2.3. F-Shape

By removing the $R2$ from the A shape, the F shape has been designed. F-shape patch is the combination of rectangles $R1$, $R3$, and $R4$. First, the simple F shape patch resonates at the centre frequency of 22.18 7 GHz with an RL value of -21.948 dB, and the bandwidth covered is (21.559–22.899) GHz. The maximum gain achieved is 7.645 dBi at 22.189 GHz. In F-shape when the MTM design is implemented, it resonates at 20.6069 GHz (20.064–21.256) GHz with the RL value of -30.4766 dB, and the maximum gain achieved is at 20.0606 GHz, i.e., 7.7348 dBi. So, the implementation of MTM improves the RL and slightly the maximum gain in the case of F-shape patch antenna. Also, in the F-shape patch with the MTM, the circular reflector has been implemented with the same radius of $R = 0.8$. Now the antenna resonates at two frequencies. The first frequency is 20.513 GHz (19.970–21.195) GHz with the RL value

Table 3. Comparative performance parameter of H shape patch.

Methodologies	Center frequencies	BW (GHz)	RL (dB)	Maximum Gain (dBi)
H shape	35.5034	1.303	−31.767	7.893
H shape+MTM	39.972, 39.134, 34.851	1.693, 2	−35.465, −12.850	8.326
H shape+MTM+Circular Reflector	39.693, 39.041, 34.572	1.777, 2.384	−26.062, −17.038, −14.081	10.684
H shape+MTM+Rectangular Reflector	38.948, 34.572	1.4, 1.833	−33.930, −14.401	10.858
H shape+MTM+Rectangular Reflector+Superstates	39.227, 39.600, 39.227, 34.851	1.55, 1.41	−24.326, −19.509, −24.326, −14.8755	12.679
H shape+MTM+Circular Reflector+Superstates	39.134, 34.758	1.341, 1.33	−33.351, −14.020	13.198

of −33.001 dB. The other resonating frequency is 24.610 GHz (24.405–24.841) GHz, and the value of RL is −11.339 dB with the maximum gain in this case 8.6710 dBi at 19.675 GHz. The RL v/s frequency and gain v/s frequency plot are given in Figures 8(a) and (b) for the F-shape patch with a comparative analysis of all methodologies. In the next step, the circular reflector is replaced with the rectangular reflector, and it resonates at two resonating frequencies of 20.2346 GHz (19.7074–20.9158) GHz and 24.4241 GHz (19.707–20.9158) GHz with the RL −32.3360 dB and −12.3553 dB, respectively, and the maximum gain achieved is 8.2752 dBi at 19.5828 GHz. Now the superstate has been implemented with the same dimensions and distance above the patch, and the resonating frequency is 24.8897 GHz (24.6917–25.063) GHz with the RL value of −24.1011 dB.

The implementation of the circular reflector with superstate resonates at 24.889 GHz (24.718–25.040) GHz with an RL value of −17.885 dB, and the maximum gain achieved is at 29.079 GHz with the value 8.4222 dBi. From Table 4, it can be seen that for the circular reflector the gain obtained is

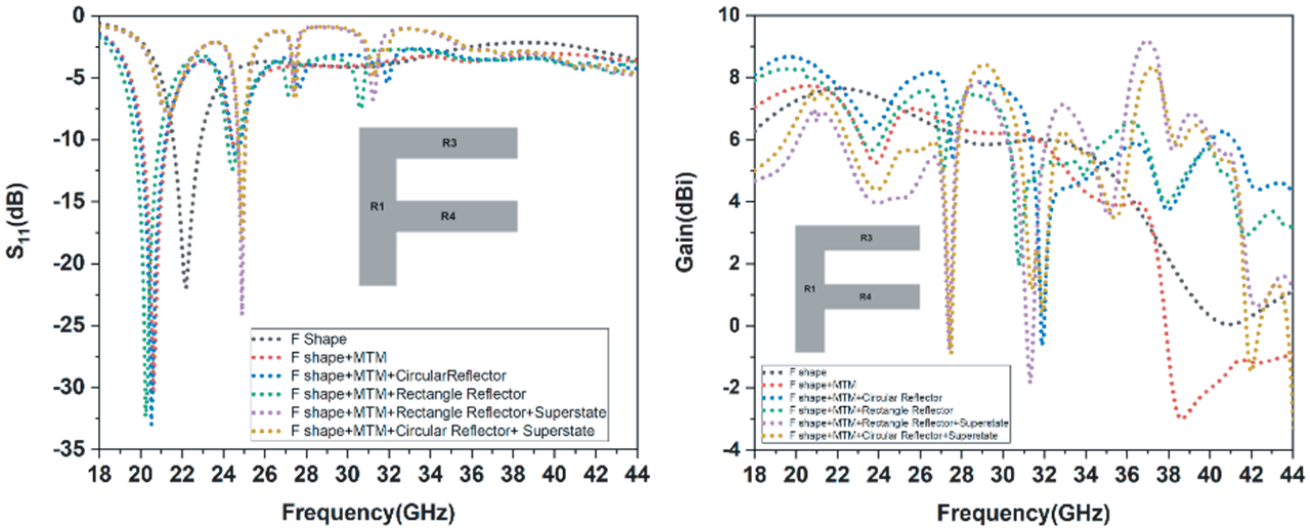

(a) (b)

Figure 8. (a) Return loss. (b) Gain comparative of F-shape patch antenna.

Table 4. Comparative performance parameter of F shape patch.

Methodologies	Center frequencies (GHz)	BW (GHz)	RL (dB)	Maximum Gain (dBi)
F Shape	22.187	1.339	−21.9481	7.6457
F shape+MTM	20.606	1.192	−30.4766	7.734
F shape+MTM+Circular Reflector	20.513, 24.610	1.22, 0.436	−33.0014, −11.339	8.670
F shape +MTM+Rectangular Reflector	20.2346, 24.4241	1.20, 0.55	−32.336, −12.3553	8.275
F shape+MTM+Rectangular Reflector+Superstates	24.8897	0.372	−24.1011	9.182
F shape+MTM+Circular Reflector+Superstates ($d2 = 3$ mm)	24.889	0.322	−17.885	8.422
F shape+MTM+Circular Reflector+Superstates ($d2 = 4.5$ mm)	24.512	0.346	−24.196	12.235

8.670 dBi, and in the F-shape patch with the circular reflector and the implementation of superstate, the gain achieved is 8.422 dBi at $d2 = 3$ mm. So, the implementation of superstate with a circular shape patch does not enhance the gain of the antenna but reduces the gain slightly at $d2 = 3$ mm. When the $d2$ value is increased up to $d2 = 4.5$ mm, the maximum gain obtained is 12.2355 dBi at the frequency of 29.3586 GHz. So, circular reflector with superstate implementation enhances the gain.

The return loss parameter in Figure 9 is shown in which the center frequency is 24.512 GHz with the RL value of −24.196 dB, and the bandwidth covered is (24.3228–24.668) GHz.

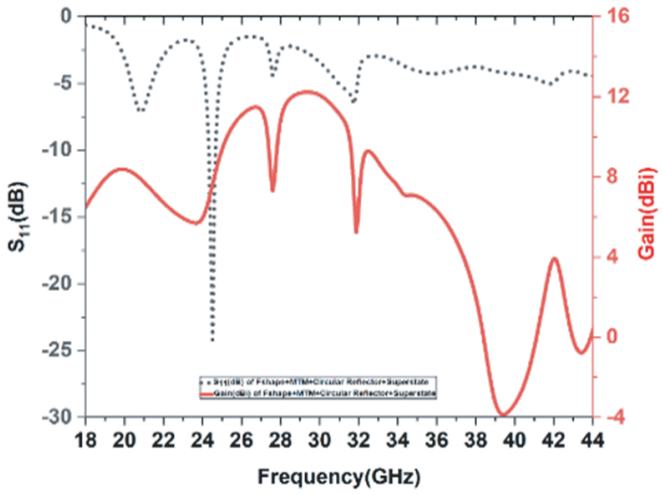

Figure 9. Return loss and gain v/s frequency.

2.4. T-Shape

The T-shape structure has been achieved by using the $R4$ and $R1$ rectangle T-shape structure in Figure 4(d) which resonates at 24.7966 GHz with $RL = -4.2677$ dB and has the RL value < -10 dB.

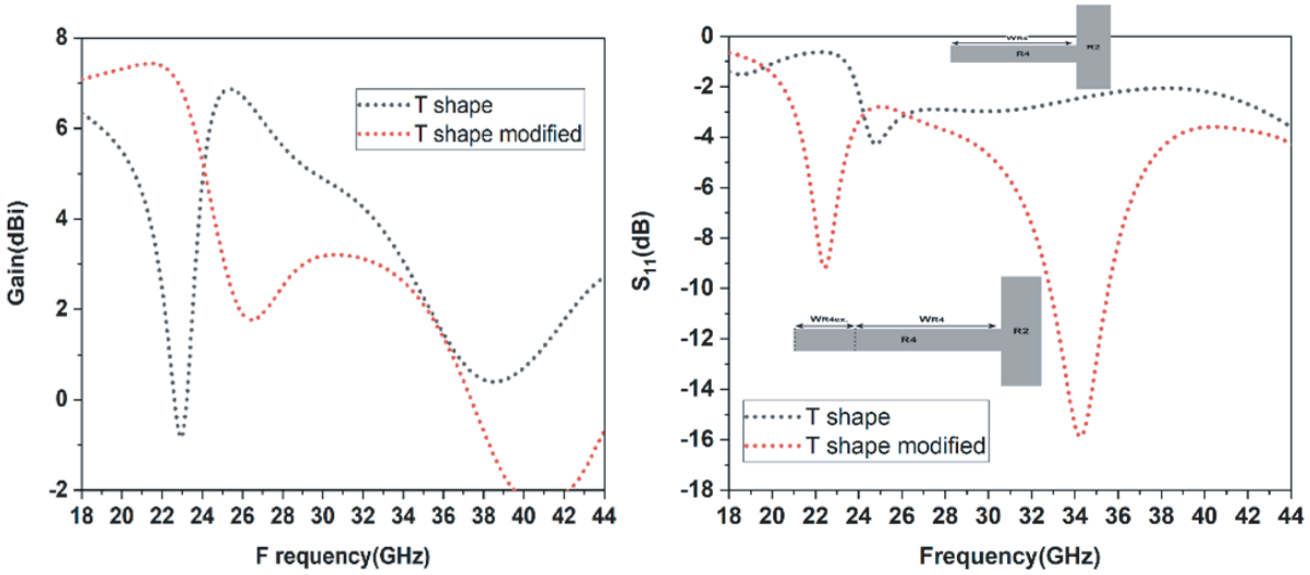

Figure 10. (a) Gain. (b) Return loss comparative of T-shape and -T modified patch structure.

Also, the maximum gain of T-shape structures is 6.8662 dBi at 25.3552 GHz. To increase the value of RL, the $WR4$ increases with the amount of $Wr4ex$. Now the T-shape modified structure given in Figure 4(e) resonates at 34.2931 GHz with the RL value of −15.871 dB covering the band (32.8408 GHz–35.547 GHz). The maximum gain attained at 21.444 GHz is 7.435 dBi. The maximum gain and RL value both increase when the $Wr4$ increases, and the plots of the RL and gain v/s frequency are given in Figures 10(a) and (b).

To improve the antenna performance characteristics, the metamaterial structure has been added similar to F-shape, A-shape, and H-shape patch antennas. T-shape modified antenna with an MTM structure resonates at 37.831 GHz, 36.527 GHz, 33.641 GHz with the return loss values −20.177 dB, −16.955 dB, −15.537 dB, respectively covering the band (32.3877 GHz–38.6011 GHz). Also, the antenna resonates at 20.6069 GHz (20.424 GHz–20.7334 GHz) with the RL value of −10.7422 dB, and the maximum gain achieved is at 19.582 GHz with 7.4383 dBi. The T-shape antenna modified with MTM resonates at 37.831 GHz, 36.527 GHz, and 33.641 GHz with the RL value of −20.177 dB, −16.955 dB, and −15.537 dB covering the band (32.3877–38.6011) GHz. Also, the fourth resonating band is 20.6069 GHz with the RL value of −10.7422 dB with the band covered from (20.424 GHz–20.733) GHz. The maximum gain was achieved at 19.5828 GHz with a value of 7.4383 dBi. Also in T-shape modified structure when the circular reflector is added, it resonates at 37.458 GHz and 36.062 GHz with RL = −34.254 dB and −23.909 dB, with the bandwidth (32.090–38.234) GHz. Along with these bands other resonating frequencies are 31.593 GHz and 20.420 GHz with RL value −10.458 dB and −11.184 dB, and covered bands are (31.478–31.711) GHz and (20.283–20.632) GHz, respectively. The maximum gain achieved is 8.7554 dBi at 8.837 GHz. In T-shape modified structure, the addition of circular reflector and MTM also increases the gain value. Now the same dimension rectangle reflector is added instead of circular reflector, and the resonating frequencies are 31.034 GHz (30.1796 GHz–32.702 GHz), 35.037 GHz (33.227–36.2535) GHz, 19.021 GHz (18.993–19.3500) GHz with the RL value of −32.663 dB, −17.093 dB, −11.670 dB, respectively. The maximum gain achieved is at 18 GHz, and the magnitude is 8.4005 dBi. With the addition of another substrate layer in the T-shape modified structure, the antenna resonates at 33.5483 GHz and 36.0621 GHz with the return loss values of −22.913 dB and −19.250 dB covering the band (32.4828 GHz–36.571) GHz. Other resonating frequencies are 37.6448 (37.3667–38.027) GHz with the RL value of −19.4217 dB and 20.8862 GHz (20.8185–20.9658) GHz with RL value of −16.0986 dB, and the maximum gain achieved is 8.3677 dBi at 36.7138 GHz. The return loss and gain v/s frequency graph are given in Figures 11(a) and (b). The same size superstate with the circular reflector resonates at the 37.5517 (37.2766–37.969) GHz and 35.969 GHz, 33.548 GHz covering the band (32.552–36.446) GHz.

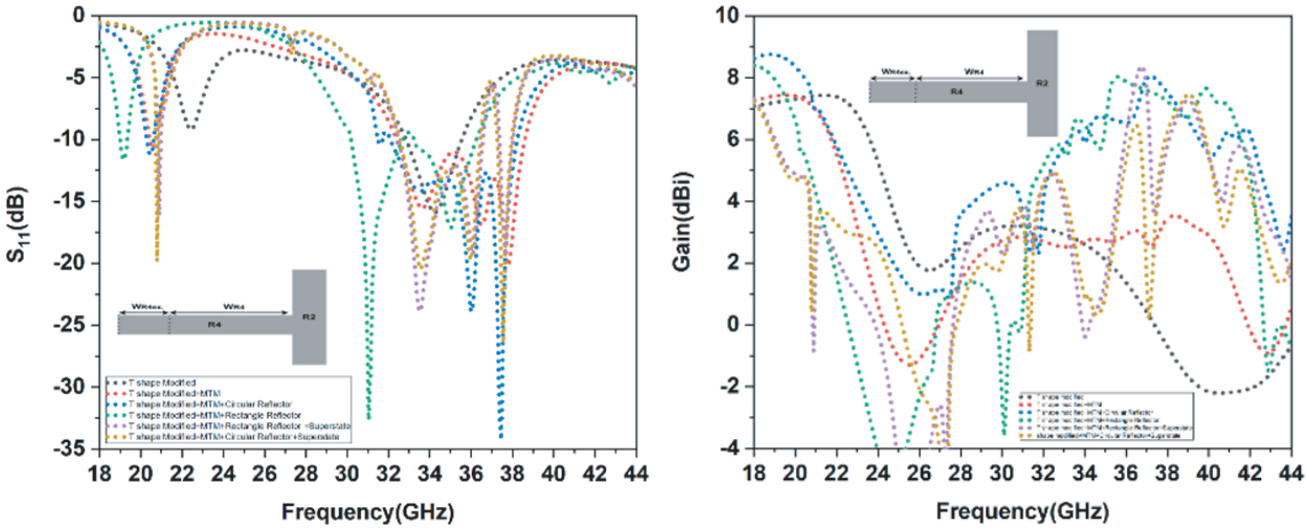

(a) (b)

Figure 11. (a) Return loss and gain comparative of T-shape modified structure.

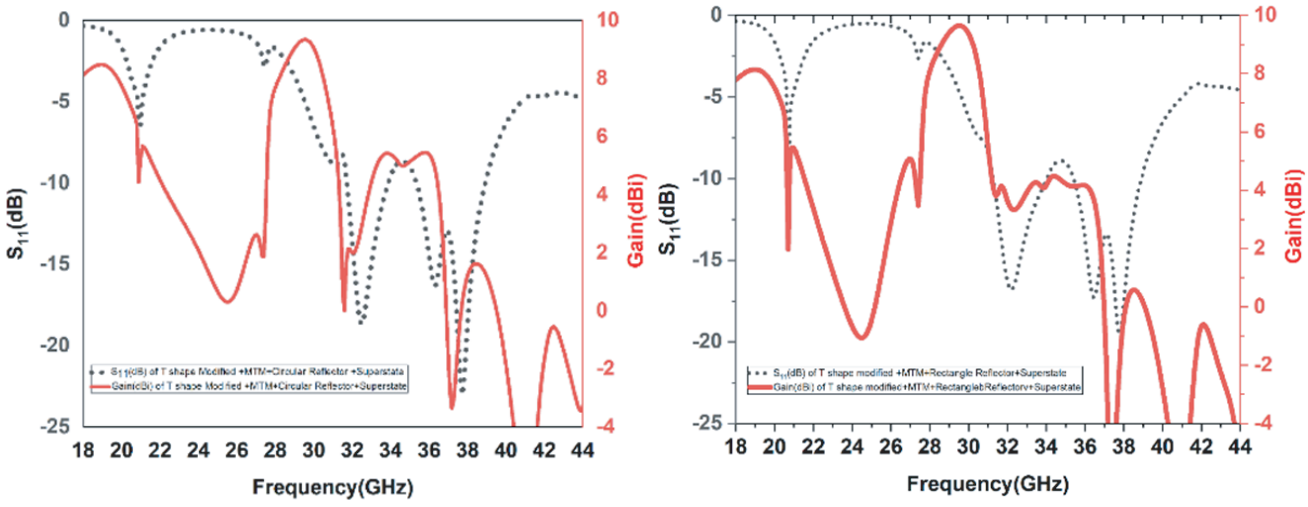

(a) (b)

Figure 12. (a) Return loss and gain v/s frequency circular reflector with superstate. (b) Return loss v/s gain frequency rectangle reflector with superstate.

Also the other resonating frequency is 20.793 GHz (20.732–20.8771) GHz with the RL values , −26.452, −19.727, −20.461, −19.823 dB, respectively and the maximum gain is 7.456 dBi at 39.041 GHz.

From Table 5 it can be seen that in circular reflector implementation the gain is 8.755 dBi. When the superstate is implemented at $d2 = 3$ mm in T-shape modified with the circular reflector the gain achieved is 7.45 dBi which is less than the only circular reflector with MTM, so when the $d2 = 4.5$ is kept in this case the maximum gain obtained is 9.3499 dBi at the frequency 29.358 GHz. Similarly, in the case of the rectangle reflector, the maximum gain achieved is 8.400 dBi. To improve the gain of the antenna, the superstate distance from the patch of the antenna has been increased from $d2 = 3$ to $d2 = 4.5$, and the gain is improved with the maximum value of 9.6506 dBi at 29.5448 GHz, which is given in Figures 12(a) and (b). In the return loss graph, the minimum value is obtained at 37.737 GHz and 36.434 GHz with the RL value of −19.538 dB and −17.307 dB, respectively, with the band covered

Table 5. Comparative performance parameter of T-shape modified shape patch.

Methodologies	Center frequencies (GHz)	BW (GHz)	RL (dB)	Maximum Gain (dBi)
T shape	34.2931	2.7	−15.871	7.435
T shape+MTM	37.831, 36.527, 33.641, 20.6069	6.21	−20.1777, −16.955, −15.537, −10.7422	7.438
T shape+MTM+Circular Reflector	37.458, 36.062, 31.593, 20.420	6.144, 0.233, 0.349	−34.254, −23.909, −10.458, −11.184	8.755
T shape+MTM+Rectangular Reflector	19.210, 31.034, 35.037	0.357, 2.523, 3.026	−11.670, −32.663, −17.093	8.4005
T shape+MTM+Rectangular Reflector+Superstates ($d2 = 3$ mm)	33.548, 36.062, 37.6448, 20.886	4.089, 0.6607, 0.146	−22.913, −19.25, −19.421, −16.098	8.3677
T shape+MTM+Rectangular Reflector+Superstates ($d2 = 4.5$ mm)	37.737, 36.434, 32.151, 20.700	3.488, 2.76, 0.083	−19.538, −17.30, −16.791, −13.790	9.6506
T shape+MTM+Circular Reflector+Superstates ($d2 = 3$ mm)	37.5517, 35.969, 33.548, 20.793	0.693, 3.89, 0.145	−26.452, −19.727, −20.461, −19.823	7.4562
T shape+MTM+Circular Reflector+Superstates ($d2 = 4.5$ mm)	37.737, 36.341, 32.524, 20.700	3.488, 2.764, 0.083	−23.006, −16.261, −18.617	9.3499

(35.4120–38.9001) GHz. Also other resonance frequencies are 32.151 GHz (31.265–34.029) GHz and 20.700 GHz (20.662–20.745) GHz with the RL of −13.790 dB, respectively.

2.5. U-Shape Patch

$R3$, $R4$, and $R1'$ are combined to design the U-shape patch structure. The $R1$ rectangle length is decreased by the value of 1.125 mm to get $R1'$. The U shape patch resonates at 23.7724 GHz with the RL value of −12.5022 dBi covering the band (23.3738–24.203) GHz. The maximum gain achieved is 6.0070 dBi at 23.213 GHz. In U-shape patch antenna when the metamaterial structure is added, it resonates at 20.6069 GHz with the RL value −12.2310 dB covering the band (20.6069–20.8847) GHz. Also, the maximum gain achieved is 7.6832 dBi at 20.6069 GHz. The U-shape structure with MTM and the circular reflector resonates at 20.606 GHz (20.261 GHz–20.937) GHz with an RL value of −13.100 dB. The maximum gain achieved is 8.561 dBi at 20.141 GHz. In the U-shape structure addition of a

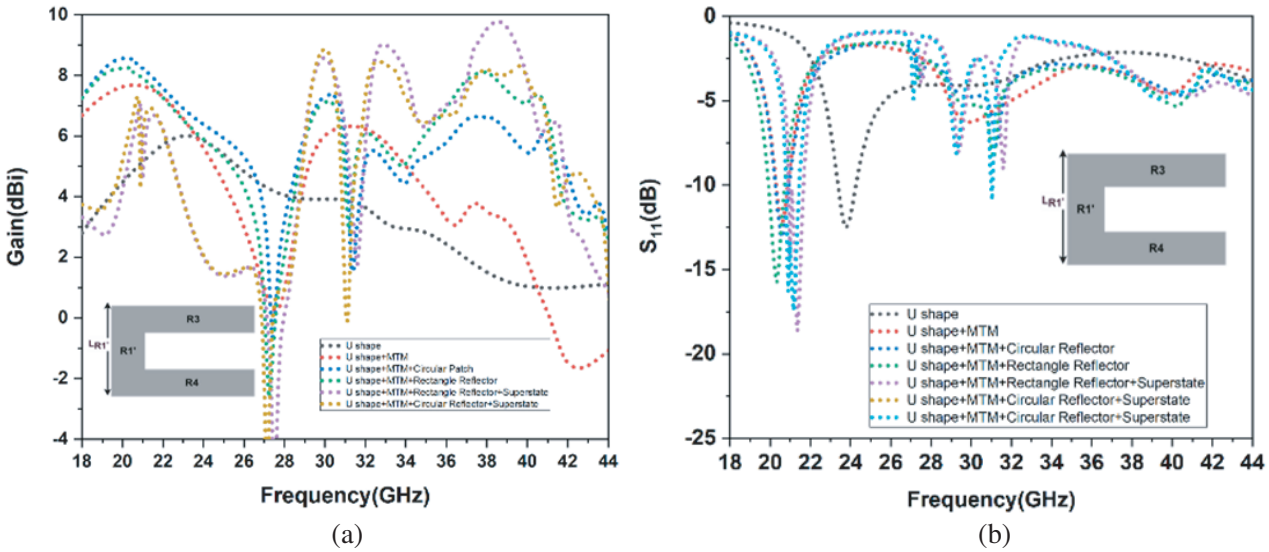

(a) (b)

Figure 13. (a) Gain and (b) return loss comparative with the implementation of all methodologies.

rectangular reflector provides the resonating frequency of 20.3276 GHz (19.9138–20.7240) GHz with the RL value of −15.7670 dB, and the maximum gain achieved is 8.249 dBi at 20.327 GHz. Also, when the superstate is added with the rectangle reflector surface, it resonates at 21.3517 GHz and 20.9793 GHz with the RL value of −18.634 dB and −14.410 dB, respectively. The frequency band covered is (20.9115–21.653) GHz, and the maximum value of gain is 9.7786 dBi at 38.575 GHz. The comparative graphs of return loss v/s frequency and gain v/s frequency are given in Figures 13(a) and (b). Also, the circular reflector with the implementation of superstate resonates at the frequencies 20.886 GHz, 21.165 GHz with RL −16.308, −17.435 dB with the band (20.791–21.442) GHz. The third resonating frequency is 31.034 GHz (30.994–31.059) GHz, and the RL value obtained is −10.900 dB with the maximum gain achieved 8.86 dBi at 30.010 GHz. The U-shape patch comparative performance parameters are given in Table 6.

The axial ratio graphs for the different shape patches like A, H, F, T, U with MTM and rectangle reflector with superstate and circular reflector with superstate are presented in Figures 14(a) and (b). The $AR < 3$ dB value shows the circular polarisation (CP) property which is useful in many applications,

Table 6. Comparative performance parameter of U-shape patch.

Methodologies	Center frequencies (GHz)	BW (GHz)	RL (dB)	Maximum Gain (dBi)
U shape	23.772	0.83	−12.5022	6.007
U shape+MTM	20.606	0.588	−12.231	7.683
U shape+MTM+Circular Reflector	20.606	0.676	−13.100	8.56
U shape+MTM+Rectangular Reflector	20.327	0.811	−15.767	8.249
U shape+MTM+Rectangular Reflector+Superstates	20.979, 21.351	0.741	−14.410, −18.634	9.778
U shape+MTM+Circular Reflector+Superstates	21.1655, 20.886, 31.034	0.651, 0.06	−17.435, −16.308, −10.900	8.86

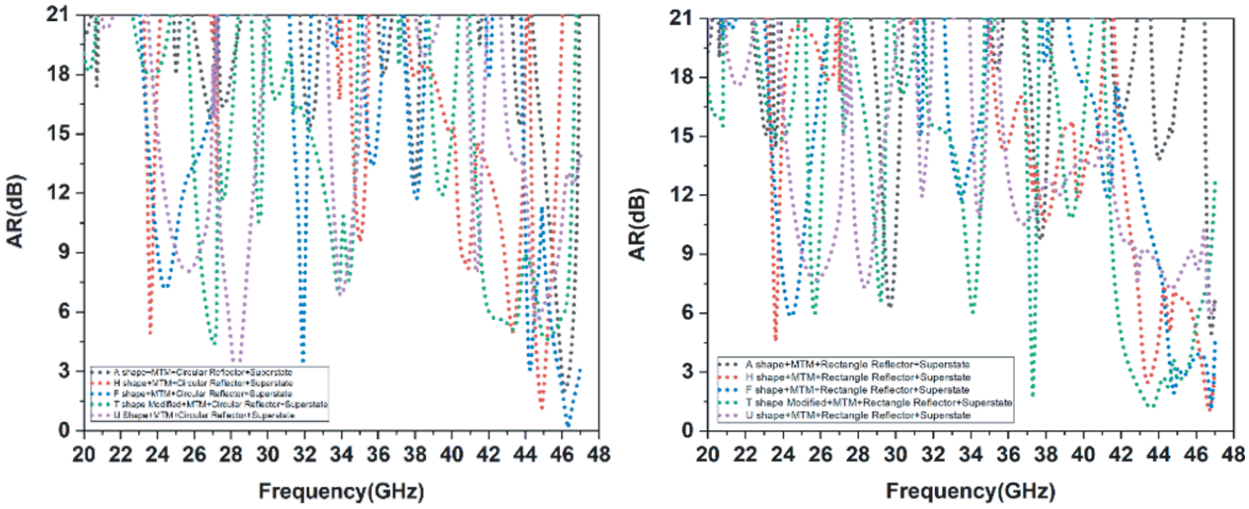

(a) (b)

Figure 14. (a) Axial ratio v/s frequency for circular reflector with superstate. (b) Axial ratio v/s frequency for rectangle reflector with superstate.

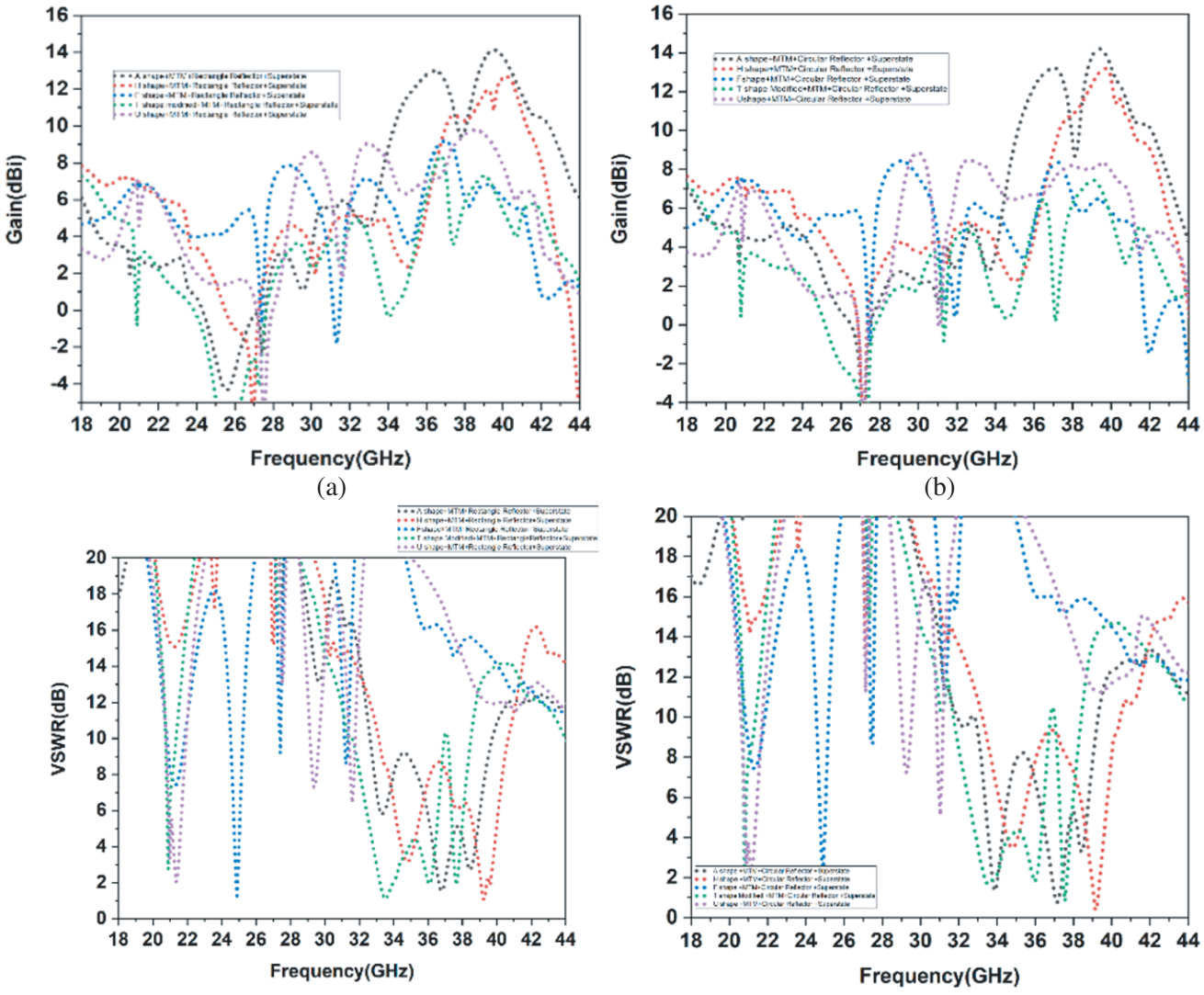

(a) (b)

(c) (d)

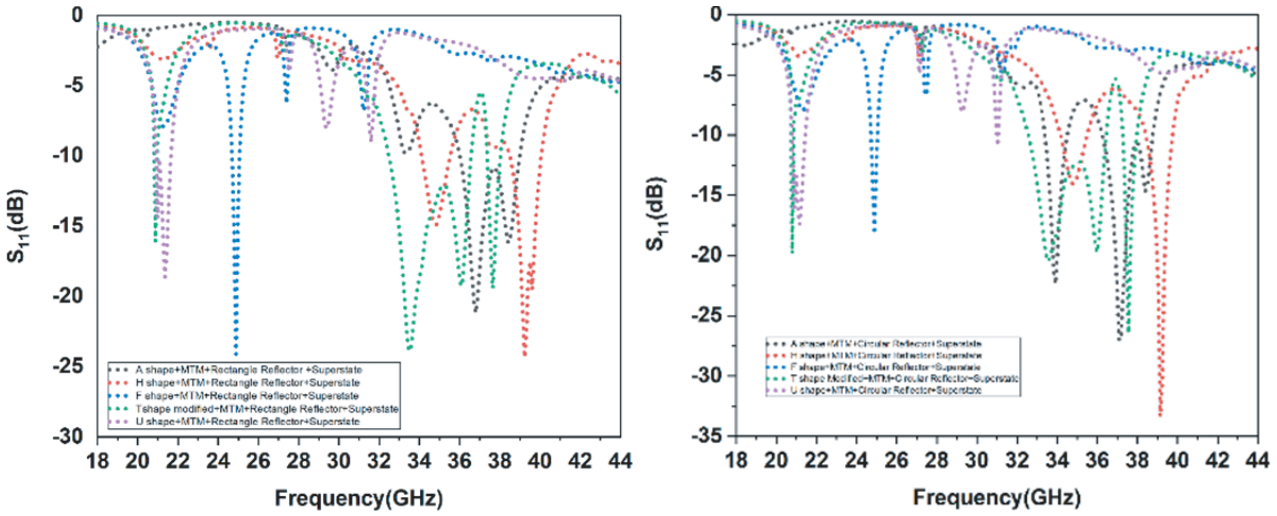

Figure 15. (a) Gain v/s frequency of rectangle reflector with superstate. (b) Gain v/s frequency of circular reflector with superstate. (c) VSWR v/s frequency of rectangle reflector with superstate. (d) VSWR v/s frequency of circular reflector with superstate. (e) Return loss v/s frequency of rectangle reflector with superstate. (f) Return loss v/s frequency of circular reflector with superstate.

so in Figures 14(a) and (b) for H-shape at higher frequencies side the $AR < 3$ dB is achieved in the frequency range (46.3612–46.9932) GHz, and another frequency band is (43.2651–43.6544) GHz. For F-shape the three bands in which the AR shows that the CP is (44.645–44.983) GHz with another two higher frequency bands (45.1772–45.524) GHz and (46.583–46.934) GHz. For T-shape modified structure, the $AR < 3$ dB bands are (42.539–44.662) GHz and (44.885–45.457) GHz. In Figure 14(a) for circular reflector H-shape patch for $R = 8$ mm, the frequency band achieved is (44.6750–45.065) GHz. For F-shape circular superstate it is (45.815–46.951) GHz, and another CP band is for the U-shape, i.e., (28.170–28.432) GHz which is the lower side of the mm-wave frequency band.

The comparative return loss, gain, and voltage standing wave ratio (VSWR) are shown in Figures 15(e), (f), (a), and (b), (c), (d). The maximum gain achieved in the case of A shape patch with the circular reflector and superstate is 14.202 dBi while in the case of rectangle reflector it is 14.130 dBi, which can be analysed in Figures 14(a) and (b).

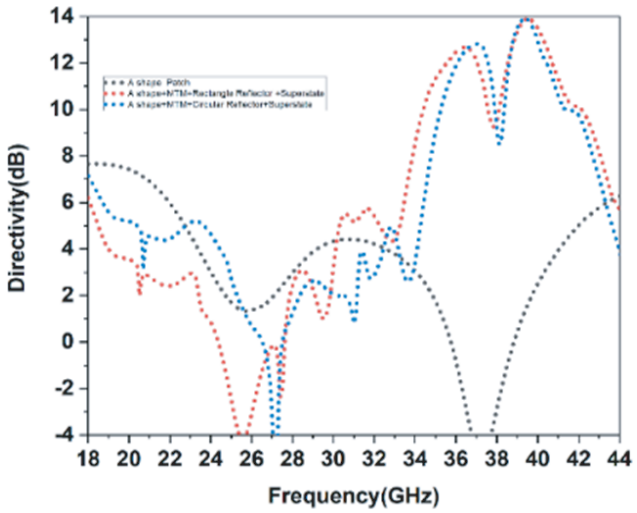

Figure 16. Directivity v/s frequency.

VSWR parameter can be seen in Figures 15(c) and (d) as (VSWR) < 2 is desirable for proper matching in different shapes patches, and it has been analysed in A-shape patch with MTM and rectangle reflector with superstate. The (VSWR) < 2 is in the frequency band (36.6321–36.9566) GHz. In Figure 15(d), A shape+MTM+circular reflector with superstate the (VSWR) < 2 BW is (38.948–39.382) GHz. The directivity enhancement is also an important aspect of the directivity improvement which can be seen in Figure 16. In the case of the A-shape patch structure, the maximum directivity is 7.669 dBi at 18.372 GHz while with the reflector surface and superstate it has been enhanced by approximately 6 dBi in both the circular reflector with superstate and rectangular reflector with superstate.

In the directivity plot Figure 17(a) and (b), the variation of directivity with the angle theta is given for the circular reflector with superstate and rectangle reflector with superstate. In Figure 17(a) at the frequency of 39.413 GHz, the maximum directivity is 13.904 dBi for circular reflector superstate and rectangle reflector superstate. The maximum directivity achieved is at 39.500 GHz with the value of 13.895 dBi. Also, the comparative literature survey is given in Table 7.

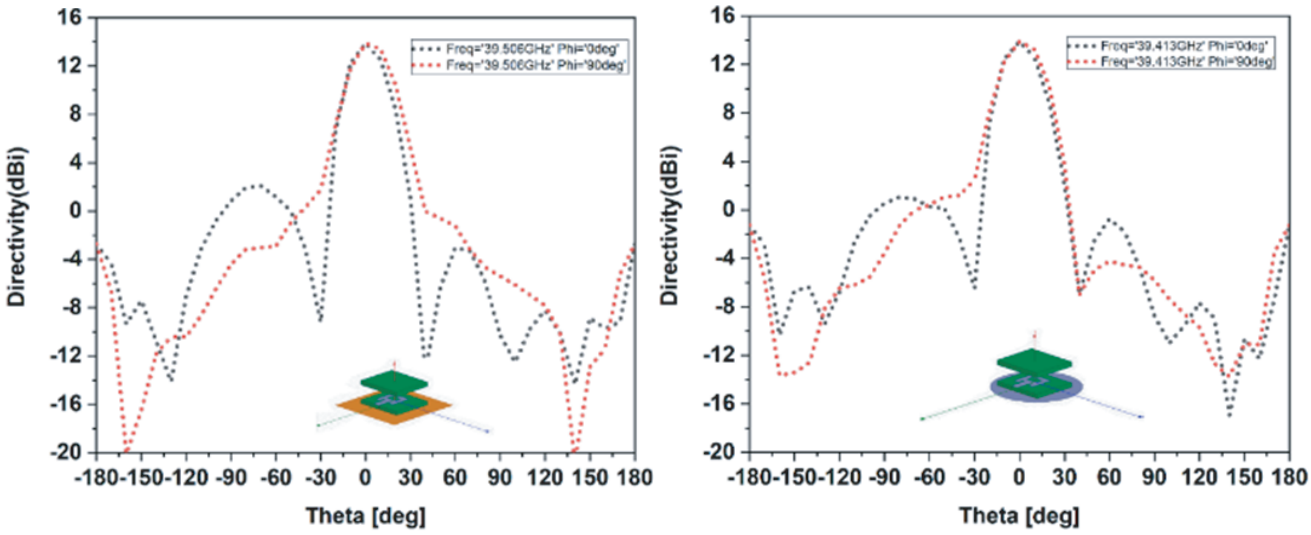

(a) (b)

Figure 17. (a) Directivity plot at phi = 0° and 90° for rectangle reflector with superstate. (b) Directivity plot at phi = 0° and 90° for circular reflector with superstate.

Table 7. Comparative literature survey with previous mm-wave antenna.

Ref.	Bandwidth (GHz)	Maximum Gain (Peak Gain) (dBi)	Size (Area) (mm × mm)
[16]	25–30	7	23 × 7
[17]	24–27.5	11	30 × 8.8
[18]	22–28.4	10.7	21.7 × 7.75
[19]	32.5–35	9.7	34 × 20
[20]	28–31	12.3	28 × 49
Proposed Structure (Rectangle Reflector)	**36.00–38.98**	**14.13**	8.4 × 9.7
Proposed Structure (Circular Reflector)	**33.38–34.50 36.24–38.76**	**14.20**	8.4 × 9.7

3. CONCLUSION

High peak gain along with dual band performance has been achieved by the implementation of MTM, reflector surface, and superstates in the proposed antenna. Also, different shape patches like H, T, U, F shapes provide different gain enhancement values with good antenna performance characteristics, and different shape patches provide different gain enhancement values by the implementation of methodologies of MTM, reflector surface, and superstates. The maximum gain value achieved in the case of A-shape patch with MTM and circular reflector with superstates is 14.2 dBi while in the case of rectangular reflector it is 14.1 dBi. Also, with the gain parameter, other antenna performance characteristics like good directivity and return loss values have been achieved. The proposed antenna is unique A-shape patch and useful for 5G mm-wave applications with the quality of overcoming the drawback of gain by achieving a high gain at mm-wave frequency.

REFERENCES

1. Rowe, W. S. T. and R. B. Waterhouse, "Reduction of backward radiation for CPW fed aperture stacked patch antennas on small ground planes," *IEEE Transactions on Antennas and Propagation*, Vol. 51, No. 6, June 2003.
2. Kurra, L., M. P. Abegaonkar, A. Basu, and S. K. Koul, "FSS properties of a uni-planar EBG and its application in directivity enhancement of a microstrip antenna," *IEEE Antennas and Wireless Propagation Letters*, Vol. 15, 1606–1609, 2016.
3. Wang, W. and Y. Zheng, "Wideband gain enhancement of high-isolation Fabry-Pérot antenna array with tandem circular parasitic patches and radial gradient PRS," *IEEE Transactions on Antennas and Propagation*, Vol. 69, No. 11, 7959–7964, 2021.
4. Javor, R. D., X.-D. Wu, and K. Chang, "Design and performance of a microstrip reflectarray antenna," *IEEE Transactions on Antennas and Propagation*, Vol. 43, No. 9, September 1995.
5. Liu, Y., N. Li, Y. Jia, W. Zhang, and Z. Zhou, "Low RCS and high-gain patch antenna based on a holographic metasurface," *IEEE Antennas and Wireless Propagation Letters*, Vol. 18, No. 3, 492–496, 2019.
6. Yang, S., Z. Yan, T. Zhang, M. Cai, F. Fan, and X. Li, "Multifunctional tri-band dual-polarized antenna combining transmitarray and reflectarray," *IEEE Transactions on Antennas and Propagation*, Vol. 69, No. 9, 6016–6021, 2021.
7. Prakash, P., M. P. Abegaonkar, A. Basu, and S. K. Koul, "Gain enhancement of a CPW-fed monopole antenna using polarization-insensitive AMC structure," *IEEE AntennasandWireless Propagation Letters*, Vol. 12, 1315–1318, 2013.
8. Liu, Z., P. Wang, and Z. Zeng, "Enhancement of the gain for microstrip antennas using negative permeability metamaterial on Low-Temperature Co-Fired Ceramic (LTCC) substrate," *IEEE Antennas and Wireless Propagation Letters*, Vol. 12, 429–432, 2013.
9. Zhou, B. and T. J. Cui, "Directivity enhancement to Vivaldi antennas using compactly anisotropic zero-index metamaterials," *IEEE Antennas and Wireless Propagation Letters*, Vol. 10, 326–329, 2011.
10. Sun, M., Z. N. Chen, and X. Qing, "Gain enhancement of 60-GHz antipodal tapered slot antenna using zero-index metamaterial," *IEEE Transactions on Antennas and Propagation*, Vol. 61, No. 4, 1741–1746, April 2013.
11. Denidni, T. A., Y. Coulibaly, and H. Boutayeb, "Hybrid dielectric resonator antenna with circular mushroom-like structure for gain improvement," *IEEE Transactions on Antennas and Propagation*, Vol. 57, No. 4, 1043–1049, April 2009.
12. Zhai, G., X. Wang, R. Xie, J. Shi, J. Gao, B. Shi, and J. Ding, "Gain-enhanced planar log-periodic dipole array antenna using nonresonant metamaterial," *IEEE Transactions on Antennas and Propagation*, Vol. 67, No. 9, 6193–6198, 2019.

13. Vaidya, A. R., R. K. Gupta, S. K. Mishra, and J. Mukherjee, "Right-hand/left-hand circularly polarized high-gain antennas using partially reflective surfaces," *IEEE Antennas and Wireless Propagation Letters*, Vol. 13, 431–434, 2014.
14. Xiong, J., Y. Hu, S. Mao, W. Zhang, S. Xiao, and B.-Z. Wang, "Agile beamwidth control and directivity enhancement for aperture radiation with low-profile metasurfaces," *IEEE Transactions on Antennas and Propagation*, Vol. 66, No. 3, 1528–1533, March 2018.
15. Zada, M., I. A. Shah, and H. Yoo, "Metamaterial-loaded compact high-gain dual-band circularly polarized implantable antenna system for multiple biomedical applications," *IEEE Transactions on Antennas and Propagation*, Vol. 68, No. 2, 1140–1144, 2019.
16. Kurvinen, J., H. Kähköne, A. Lehtovuori, J. Ala-Laurinaho, and V. Viikari, "Co-designed mm-wave and LTE handset antennas," *IEEE Transactions on Antennas and Propagation*, Vol. 67, No. 3, 1545–1553, 2019.
17. Rodriguez-Cano, R., S. Zhang, K. Zhao, and G. F. Pedersen, "Reduction of main beam-blockage in an integrated 5G array with a metal-frame antenna," *IEEE Transactions on Antennas and Propagation*, Vol. 67, No. 5, 3161–3170, May 2019.
18. Rodriguez-Cano, R., S. Zhang, K. Zhao, and G. F. Pedersen, "Mm-wave beam-steerable endfire array embedded in slotted metal-frame LTE antenna," *IEEE Transactions on Antennas and Propagation*, Vol. 68, No. 5, 3685–3694, 2020.
19. Cheng, Y. J. and Y. Fan, "Millimeter-wave miniaturized substrate integrated multibeam antenna," *IEEE Transactions on Antennas and Propagation*, Vol. 59, No. 12, 4840–4844, December 2011.
20. Di Paola, C., K. Zhao, S. Zhang, and G. F. Pedersen, "SIW multibeam antenna array at 30 GHz for 5G mobile devices," *IEEE Access*, Vol. 7, 73157–73164, 2019.